Effects of alternative marine diesel fuels on the exhaust particle size distributions of an off-road diesel engine.

Author: Ovaska, Teemu; Niemi, Seppo; Sirviö, Katriina; Nilsson, Olav; Portin, Kaj; Asplund, Tomas

Title: Effects of alternative marine diesel fuels on the exhaust particle size distributions of an off-road diesel engine.

Year: 2019

Version: Accepted manuscript

Please cite the original version:

Ovaska, T., Niemi, S., Sirviö, K., Nilsson, O., Portin, K., & Asplund, T., (2017). Effects of alternative marine diesel fuels on the exhaust particle size distributions of an off-road diesel engine. *Applied thermal engineering* 150, 1168–1176. https://doi.org/10.1016/j.applthermaleng.2019.01.090

Effects of alternative marine diesel fuels on the exhaust particle size distributions of an off-road diesel engine

Teemu Ovaska [a,*], Seppo Niemi [a], Katriina Sirviö [a], Olav Nilsson [a], Kaj Portin [b], Tomas Asplund [b]

[a] School of Technology and Innovations, University of Vaasa, P.O. Box 700, FI-65101 Vaasa, Finland

[b] Wärtsilä Corporation, FI-65101 Vaasa, Finland

* Corresponding author: teemu.ovaska@univaasa.fi

HIGHLIGHTS

- Renewable naphtha-light fuel oil blend decreased the accumulation mode particles
- The blend emitted either less or more particles than light fuel oil depending on load
- Circulation-origin marine gas oil and kerosene generated a high total particle number

KEYWORDS

Diesel engine, exhaust particle number, alternative fuel, light fuel oil

ABSTRACT

The main objective of this study was to find out how alternative fuels affect the exhaust gas particle size distribution. The fuels are later intended for marine applications. Along with low-sulfur marine light fuel oil (LFO), a high-speed off-road diesel engine was fueled by circulation-origin marine gas oil (MGO), rapeseed methyl ester (RME), crude tall oil derived renewable diesel (HVO), the 20/80 vol.-% blend of renewable naphtha and marine LFO, and kerosene. Particle size distributions were measured by means of an engine exhaust particle sizer (EEPS), but soot, gaseous emissions and the basic engine performance were also determined. During the measurements, the 4-cylinder, turbocharged, intercooled engine was run according to the non-road steady cycle complemented by an additional load point. The engine control parameters were kept constant, and any parameter optimization was not made with the studied fuels.

Relative to baseline LFO, both naphtha-LFO blend and RME reduced particle numbers above the size range of 50 nm. Circulation-origin MGO and kerosene generated a high total particle number (TPN), most likely due to their higher sulfur contents. MGO and RME were beneficial in terms of carbon monoxide (CO) and hydrocarbon (HC) emissions while nitrogen oxide (NO_x) emissions were the highest with RME. The differences in smoke emission were negligible.

1. Introduction

International shipping produces 5–10% of the total global sulfur emissions [1]. Along with the oxides of sulfur (SO_x) and particles, the carbon dioxide (CO_2) and NO_x emissions, have also to be reduced significantly in order to inhibit the pollution of the earth atmosphere. As an act for the pollution inhibition, the emissions of shipping are considerably regulated worldwide via the MARPOL Annex VI convention of the International Maritime Organization (IMO). These regulations aim to progressively reduce the emissions of SO_x and NO_x. Even outside the Sulfur Emission Control Areas (SECAs), fuel sulfur content has to be under 0.5% in 2020. [2].

Marine sulfur emissions originate mainly from large marine diesel engines, where heavy fuel oil (HFO) is widely combusted. As a residual fuel, HFO has high sulfur and ash contents. The high sulfur content and other fuel characteristics have also been reported to affect the marine exhaust particle emissions. [3,4].

Diesel engine exhaust particles form the size distribution with two distinctive particle modes; accumulation mode and nucleation mode [5,6,7,8]. The particle mean diameters in nucleation mode are under 50 nm [9], whereas the mean diameter range in soot mode is 50–500 nm [5,10]. Particle number (PN) and mass emissions can be decreased through developing the engine design, exhaust gas after treatment systems, and fuels. Compared to new engine designs or after treatment solutions, alternative liquid fuels can be taken in use relatively rapidly by the operators. Alternative fuels can also offer immediately realizable air quality improvements, and in addition to a SO_x emission decline, the low sulfur content of these new fuels is beneficial for the performance of diesel particulate filters (DPF) [11,12]. Filters, and even

more efficient emissions reduction technologies are needed soon. For the first time, the new emission stage (Stage V) also has the limits for the exhaust particle number emissions of the off-road engines, including inland waterway vessels. This regulation of the European Commission and the Council comes gradually into effect within 2019–2020. [13].

Ship owners can meet the emission regulations, especially the IMO's SO_x limitation, by using low-sulfur fuel oils, liquefied natural gas (LNG), or exhaust gas scrubbers. Likely therefore, the low-sulfur fuel oils and other alternative fuel options are going to be used increasingly instead of HFO. Light fuel oils, such as marine diesel oil (MDO) or MGO, are already used in small vessels and the marine auxiliary diesel engines of large ocean-going ships. In Finland, for example, low sulfur marine fuels and LNG have been substitutes for bunkered HFO already for a certain time. [1,14,15].

Sustainable and affordable alternative liquid fuels are, however, also needed for the compression ignited (CI) engines. Florentinus et al. [16] assessed qualitatively the technical compatibility of various biofuels in marine engines. Mono-alkyl-esters of long-chain fatty acids, i.e. fatty-acid methyl esters (FAME), di-methyl ether (DME), straight-, and hydrotreated vegetable oils (SVO, HVO) are suitable liquid fuels for both high-speed and medium speed engines [16]. Moreover, Finnish HVO, as studied e.g. by [17], could also be a potential option for medium speed engines.

Moreover, the US Army Single Fuel Forward Policy raised interest to study jet fuels in CI engines which are used in different kind of military vehicles. The aircraft gas turbine engines have been previously run with Jet Propellant 4 (JP-4) fuel which has been replaced by the low sulfur JP-8 fuel, similar to kerosene-based Jet A-1 fuel of the commercial aviation. Jet A-1 fuel has been identified to have same kind of properties than diesel fuel oils (DFO) or low-sulfur LFO. [18]

However, the alternative fuel option has to also be compatible with the other systems in ship. With e.g. FAME, several issues have to be considered, like a tendency to oxidation during long term storage, affinity to water and risk of microbial growth, degraded low temperature flow properties, and material deposition on exposed surfaces, including filter elements. The problems may arise especially with over 20 vol.-% blends of FAME. [16]. Kerosene-based jet fuel has typically lower cetane number and viscosity

compared to LFO, MGO or MDO used in the CI engines in marine and land-use applications. Low cetane number extends the length of the ignition delay, which affects the combustion timing. Extended delay leads to the changes of cold-starting performance, combustion noise level, and exhaust emissions. Due to low fuel viscosity, the fuel injection system performance can deteriorate and the fuel pump wear and leakage may occur. [18].

This paper presents how the selected alternative marine fuels affected exhaust gas particle size distributions in the study which was the first stage of a large marine fuel research project. Circulation-origin marine gas oil (MGO) and a blend of renewable naphtha and marine light fuel oil (LFO) were selected to this study because both fuels are novel marine fuel options. Both could meet the sustainability and affordability goals set by the ship owners. Along with these fuels, the other studied low-sulfur fuels were LFO, rapeseed methyl ester (RME), crude tall oil derived renewable diesel (HVO), and kerosene. High-speed engine experiments were conducted before going to medium-speed engine tests. Alongside the exhaust gas particle number and size distributions, the exhaust smoke, gaseous emissions and basic engine performance were determined. The blend fuel contained 20 vol.-% of naphtha and 80 vol.-% of LFO whereas neat LFO was used as the reference fuel. The high-speed off-road diesel engine was driven according to the non-road steady cycle (NRSC) plus at one additional load point. During the experiments, the default engine control parameters were kept constant, and no parameter optimization was applied with the studied fuels.

2. Experimental setup

2.1. Engine and fuels

The experiments were performed with a diesel engine installed in a test bed and loaded by an eddy-current dynamometer. The running cycle was the ISO 8178 C1, added by the 25% load point at intermediate speed.

The 4-cylinder test engine was a turbocharged, intercooled (air-to-water) off-road diesel engine, equipped with a common-rail fuel injection system. The displacement of the engine was 4.4 dm^3 (bore 108

mm, stroke 120 mm) and the rated power 101 kW. The engine was not equipped with any exhaust gas after-treatment devices. The engine lubricating oil was Valtra Engine CR-4 10W-40.

In addition to baseline LFO, the effects of naphtha-LFO blend, MGO, HVO, RME, and kerosene on the exhaust gas particle size distribution were investigated. Naphtha-LFO blend contained 20 vol.-% of naphtha. Naphtha was a side-product of wood-based renewable diesel production. MGO was a Finnish marine fuel produced from recycled lubricating oils. Kerosene was Jet A-1 type aviation fuel. For the fuels, cetane number, density, sulfur content and kinematic viscosity at 40 °C were analyzed by the fuel laboratory of the University of Vaasa. Table 1 shows the all analyzed fuel properties. The values for the fuel polyaromatic content are based on the available literature in Table 1. Based on the information received from the fuel supplier, naphtha may contain negligible traces of polyaromatic compounds. Nevertheless, the polyaromatic content of naphtha-LFO blend can still be assumed to meet the SFS-EN 590:2013 standard.

2.2. Analytical procedures

The particle number and size distribution, soot, gaseous emissions and residual oxygen content were measured in the laboratory conditions and sampled from the raw engine exhaust. The air mass flow rate

Table 1. Fuel specifications.

Parameter	Method	LFO	MGO	RME	HVO	Naphtha-LFO	Kerosene	Unit
Cetane number	EN 15195	52	68	53	65	51	41	-
Density (15 °C)	EN ISO 12185 / ASTM D7042	827	843	883	813	805	787	kg/m^3
Sulfur content	EN ISO 20884 / EN ISO 20846	8.3	< 100	< 5	< 5	6.8	1000	mg/kg
Kin. viscosity (40 °C)	EN ISO 3104 / ASTM D7042	1.84	7.69	4.49	3.5	1.37	0.94	mm^2/s
Polyaromatics		< 8[a]	0.9[b]	0[c]	0.2[d]	< 8[a]	< 26.5[e]	wt.-%

[a] The maximum allowable polyaromatic content of the fuel standard EN590 [19].
[b] Analyzed by the fuel supplier.
[c] [20].
[d] [17].
[e] The maximum allowable polyaromatic content of the fuel manufacturer [21].

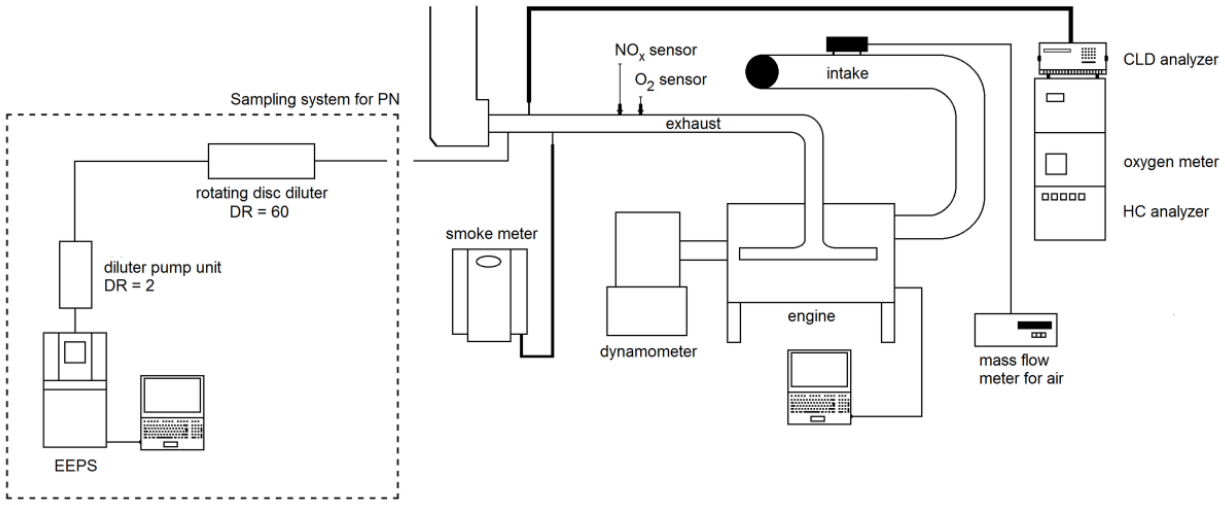

Fig. 1. Experimental setup.

was measured from the intake air duct of the engine. Each day before the measurements, the analyzers were calibrated manually once a day according to the instructions of the instrument manufacturers. The experimental setup is in Fig. 1.

The particles from a size range of 5.6 to 560 nm were measured by an engine exhaust particle sizer (EEPS, model 3090, TSI Inc.), for which the sample flow rate was adjusted at 5.0 l/min. The "SOOT" inversion was applied in the EEPS data processing [22]. The exhaust sample was first diluted with ambient air by a rotating disc diluter (RDD) (model MD19-E3, Matter Engineering AG). The dilution ratio used in the RDD was constant 60. The exhaust aerosol sample was conducted to the RDD and a dilution air was kept at 150 °C. The diluted sample (5 lpm) was further diluted by purified air with a dilution ratio of 2. Thus, the total dilution ratio was 120.

The particle number (PN) was recorded consecutively three times. Each recording was one-minute long. One-minute stable time periods were chosen for the results recordings of the PN and particle size distributions. The averaging interval of 2 seconds was used for every period. The average PN values, calculated from the recordings, were multiplied by the dilution ratio of the exhaust sample. The uncertainty

of the PN measurement was approximated by calculating the standard deviation of the PN averages, taken from each one-minute recording. The recorded smoke value was the average of three consecutively measured smoke numbers (model 415S, AVL). Nitrogen oxides (NO_x), hydrocarbons (HC) and carbon monoxide (CO) were measured by an Eco Physics CLD 822Mh, J.U.M. VE7, and Siemens Ultramat 6, respectively.

The sensor data were collected by means of software, made in the LabVIEW system-design platform. In addition to the gaseous emissions, the systems recorded the temperatures of cooling water, intake air and exhaust gas plus the pressures of the intake air and exhaust gas. The engine control parameters were followed via WinEEM4 engine management software.

2.3. Experimental matrix and running procedure

The measurements were conducted according to the eight-point test cycle C1 of the ISO 8178-4 standard, known as NRSC, Table 2. The rated speed of the engine was 2200 rpm and the intermediate speed was chosen to be 1500 rpm. Additionally, the measurements were taken at 25% load (3.2 bar) at intermediate speed. With the low-viscosity kerosene, the default engine control parameters made the engine running possible only at intermediate speed. Because no engine parameter optimization was applied during the experiments, the additional load point was chosen to gather more information about the effects of kerosene on the exhaust particle size distribution. An eddy-current dynamometer of model Horiba WT300 was employed to load the engine.

Table 2. Experimental matrix [23].

Point	1	2	3	4	5	6	7	8
Speed	Rated				Intermediate			Idle
Load (%)	100	75	50	10	100	75	50	0
Torque (Nm)	351	263	176	35	450	338	225	0
BMEP (bar)	10.0	7.5	5.0	1.0	12.9	9.7	6.4	0

A canister of 30 liters was used as a fuel tank. After the tests with each fuel were completed, the fuel filter was emptied, and the engine was run with new fuel for 10 minutes. At each load point, the intake air temperature was adjusted at 100 °C downstream the charge air cooler to also ensure proper ignition for low cetane fuels. The temperature was controlled manually by regulating cooling water flow to the heat exchanger. Before the recordings, it was waited that the engine had stabilized, the criteria being that the temperatures of coolant water, intake air and exhaust were stable. The length of the measurement period was not tied to a certain time.

The particle number and size distribution were recorded continuously at each load point. For each fuel, engine warm up and measurements were performed in an exactly similar way.

3. Results

3.1. Particle size distributions

Generally at rated and at intermediate speed, naphtha-LFO blend and RME reduced particle numbers within the size range of 37 to 200 nm compared to LFO while kerosene and methyl ester showed higher particle numbers within the size range of 8–13 nm than the other fuels. At this range, HVO was favorable at intermediate speed and at low idle. Below, the distributions are examined more thoroughly at certain loads.

Fig. 2 shows the particle size distributions at full load at rated speed. The distribution was bimodal, like at many other loads, one peak being detected at a particle size of 10 nm and the other within a size range of 30 to 60 nm. At the size of approx. 10 nm, the least particles were observed with HVO and LFO. Between 14 and 340 nm, the smallest particle numbers were recorded with RME, while MGO produced the highest PN.

At 75% load at rated speed, a bimodal distribution was also detected with all fuels, Fig. 3. While the particle number was clearly the lowest for LFO at 10 nm, RME emitted the least particles within the size range of 37 to 260 nm, as at full load. MGO emitted a high PN within the entire size range. The nucleation mode particles were also high with RME.

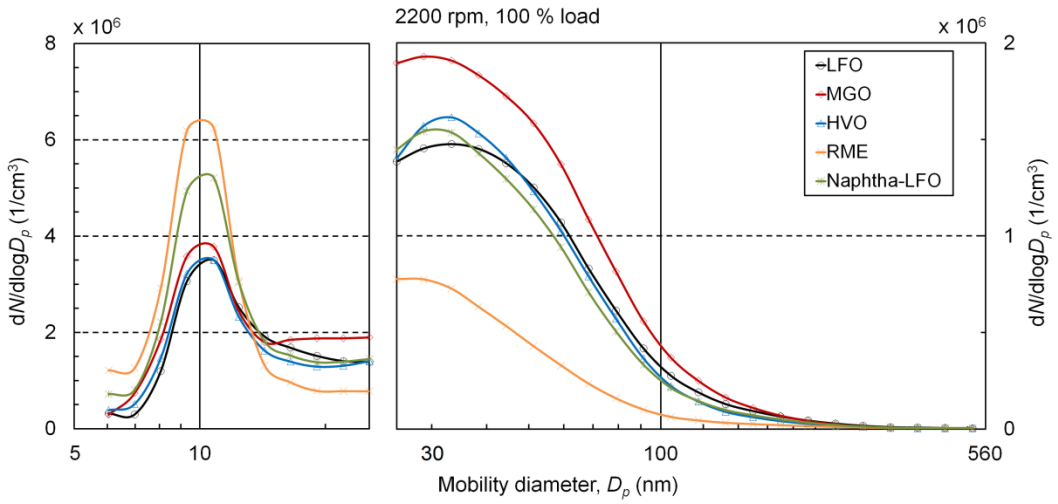

Fig. 2. Exhaust particle size distributions at full load at rated speed for different fuels. It should be noted that the left and right scales of the y axes are different.

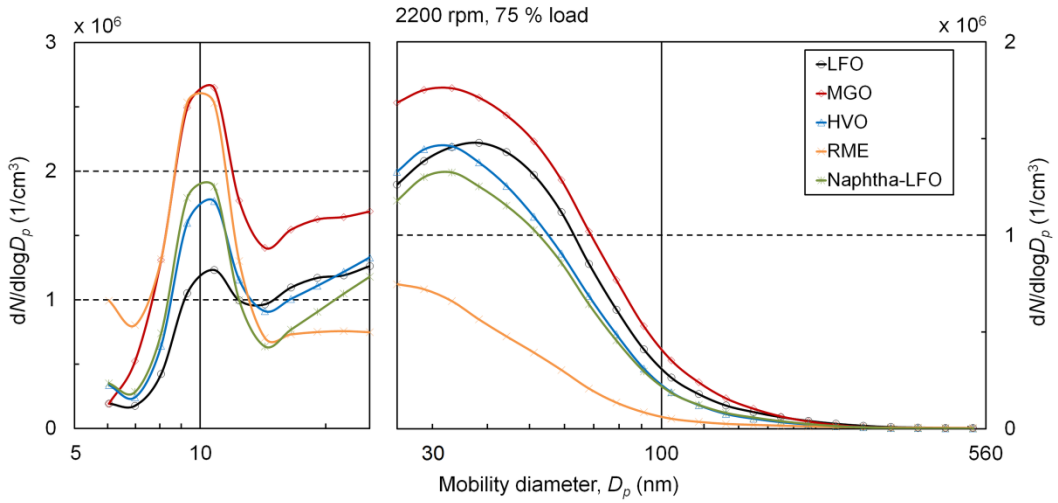

Fig. 3. Exhaust particle size distributions at 75% load at rated speed for studied fuels. Please note the different scales of the y axes.

For full and half loads at intermediate speed, the particle size distributions are illustrated in Figs. 4 and 5. Again, there was one peak at a particle size of approx. 10 nm and the other within the size range of 30 to 60 nm. The least particles between 37 and 260 nm were detected with RME.

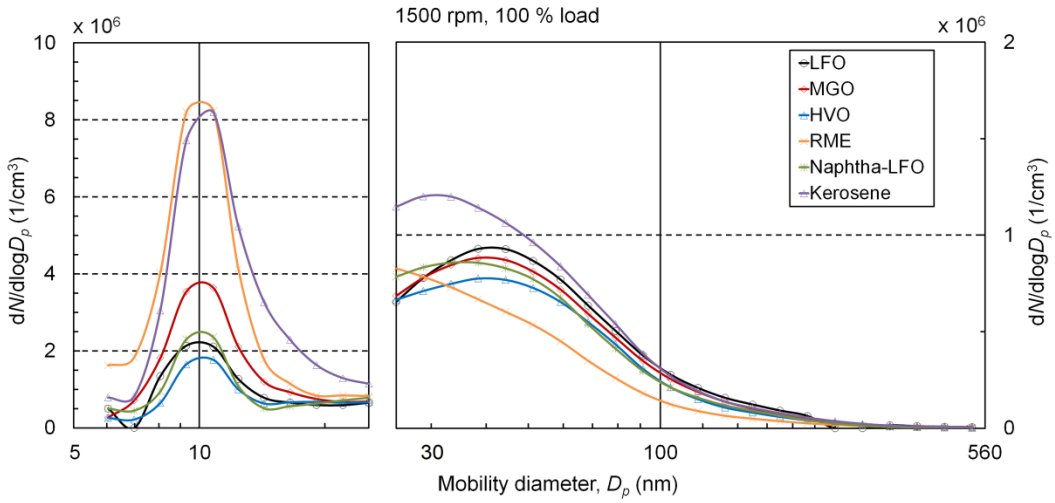

202

203 **Fig. 4.** Exhaust particle size distributions at full load at intermediate speed for different fuels. Please note

204 the different scales of the y axes.

205

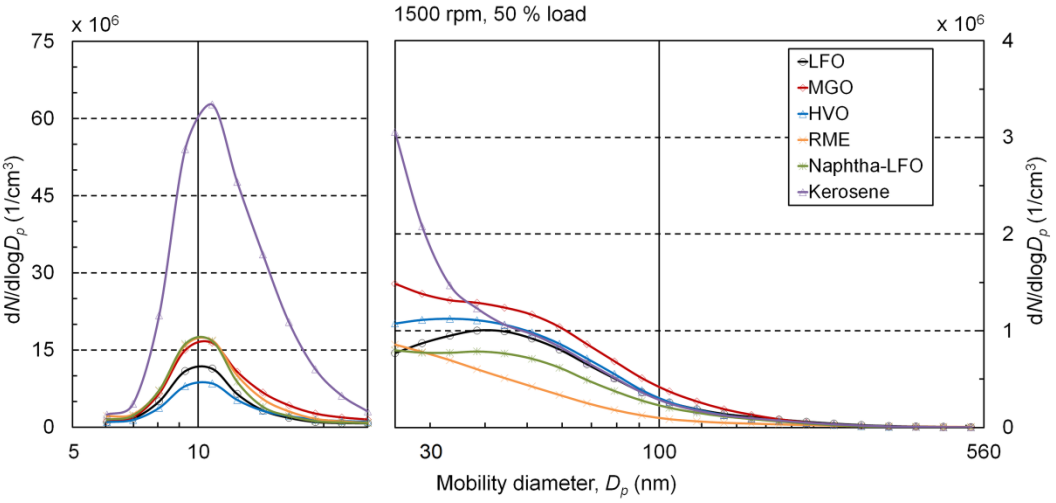

206

207 **Fig. 5.** Exhaust particle size distributions at half load at intermediate speed for studied fuels. Please note

208 the different scales of the y axes.

209

210 As at rated speed, the use of naphtha-LFO blend reduced again particle numbers within the size range

211 of 37 to 200 nm compared to neat LFO. At full load, RME and kerosene produced the most particles at the

212 size category of 10 nm while HVO showed the lowest PN. At this category at half load, the PN was far the

highest with kerosene and again the lowest with HVO. At intermediate speed, relative to other fuels, the MGO results were slightly more favorable than at rated speed.

Both at rated and intermediate speeds, the biggest differences in the PN emissions were detected at the particle size of approx. 10 nm, either HVO or LFO generating mostly the lowest particle numbers. Kerosene, only used at intermediate speed, produced often the highest amount of particles at 10 nm. At intermediate speed, the distribution shapes differed from those at rated speed since the peaks between 30 and 60 nm were now much lower compared to those at approx. 10 nm.

The measured total particle number (TPN, from 5.6 to 560 nm) is shown at rated speed in Fig. 6 and at intermediate in Fig. 7. For all fuels at rated speed, the TPN decreased when the load decreased from full to 75% load and remained then almost constant at half load. It increased, however, when the load decreased further, being clearly the highest at 10% load.

At full and 10% loads, the TPN were the lowest when HVO was used. At other loads at rated speed, RME had the lowest TPN. As a whole, naphtha-LFO blend was very competitive with neat LFO. MGO generated the highest TPN at all loads at rated speed.

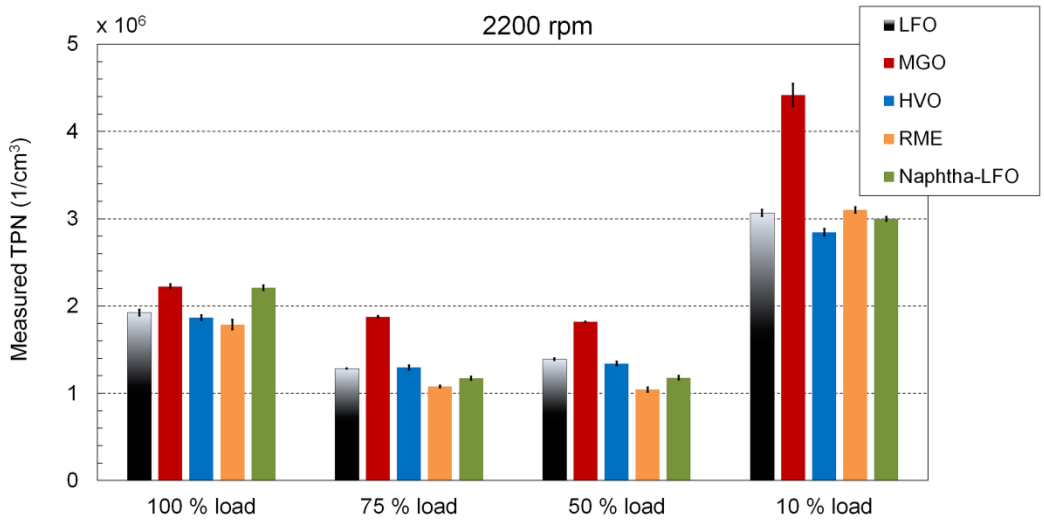

Fig. 6. Measured TPN at rated speed.

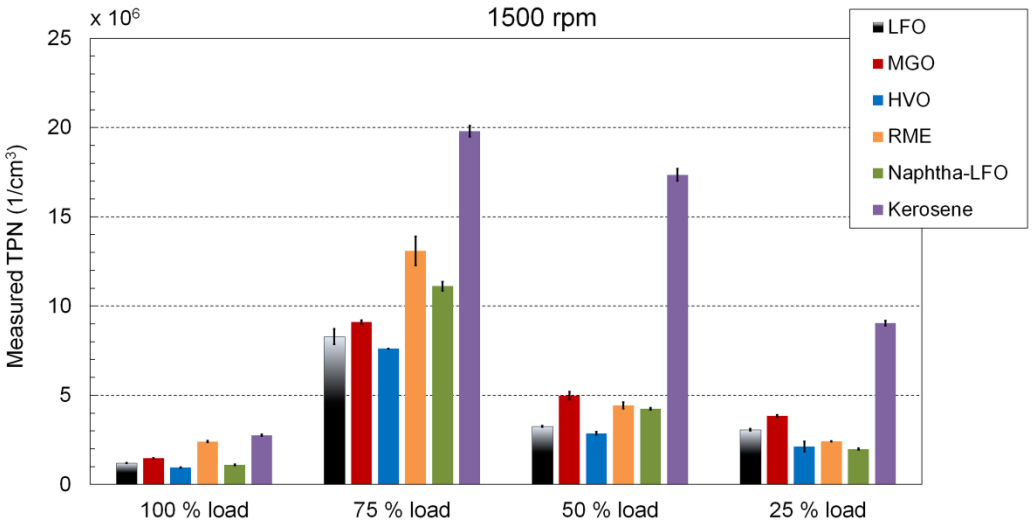

Fig. 7. Measured TPN at intermediate speed.

At intermediate speed, the TPN was at the lowest at full and the highest at 75% load. The TPN decreased when the load decreased from 75 to 25%. Regardless of load, HVO generated the lowest TPN whereas kerosene showed the highest. At some loads, naphtha-LFO generated a higher TPN than LFO, at other loads a lower one. MGO resulted again in a somewhat higher TPN than LFO.

The measured TPN was divided into two categories depending on how many of the particles out of TPN were detected below or above the size category of 23 nm. The shares of the particles above the size of 23 nm were calculated for the fuels, Table 3. At full load at rated speed, 40% of the particles were detected above the size of 23 nm, and thus, 60% below. The lowest average share of the particles above 23 nm was detected with RME, and the highest share with HVO. At 75% load at intermediate speed, the shares of the particles above 23 nm were only 4.3–5.8%.

3.2. Gaseous emissions and smoke

Table 4 shows the brake specific emissions of HC, NOx, and CO and smoke number ranges. In general, MGO and RME were favorable in terms of CO and HC emissions while NOx emissions were the lowest

247 with HVO. The smoke numbers were altogether minor with all fuels. Due to the intended use of an SCR
248 catalyst, high NOx tuning of the test engine had most likely a decreasing effect on smoke.
249
250 **Table 3.** The share of particles larger than 23 nm out of the TPN for all fuels at different loads.

Speed	Rated				Intermediate			Idle
Load (%)	100 %	75 %	50 %	10 %	100 %	75 %	50 %	0 %
LFO	40	59	58	57	44	5.6	17	7.2
MGO	44	48	51	36	34	5.5	15	8.0
HVO	41	50	55	53	46	5.8	21	22
RME	18	27	34	30	15	4.5	7.2	20
Naphtha-LFO	33	53	57	55	43	4.3	10	7.9

251
252 **Table 4.** Cycle-weighted brake specific emissions of HC, NO_x and CO and smoke number ranges from
253 lowest to highest within the NRSC cycle with different fuels. The specific PN emission was determined
254 over the size range of 5.6–560 nm.

	HC (g/kWh)	NO_x (g/kWh)	CO (g/kWh)	Smoke (FSN)
LFO	0.24	9.3	0.33	0.014–0.038
MGO	0.16	9.3	0.28	0.014–0.033
HVO	0.20	8.9	0.32	0.013–0.031
RME	0.12	10.8	0.30	0.005–0.015
Naphtha-LFO	0.29	-	0.36	0.011–0.031

255
256 **4. Discussion**
257 In the present study, all particle size distributions measured from the exhaust gas of the high-speed
258 off-road diesel engine had a bimodal shape. This common shape of engine-out size distributions has also
259 been observed both in on-road and laboratory conditions in case of heavy-duty diesel truck [24], light-duty
260 diesel [7], natural gas buses [25], direct-injected gasoline vehicle [26,27] and off-road diesels [17,28–30].

Moreover, Ntziachristos et al. [31] detected bimodal particle size distributions in the exhaust gas of a medium-speed marine diesel engine when LFO was used at low load.

The nucleation mode particles have a non-volatile core which is considered to initiate in the cylinder or in the tailpipe [9,32]. The most of the nucleation mode particles are believed to form during dilution of the exhaust gas. Their formation has been reported to be sensitive to the engine parameters [33], fuel and lubricant oil characteristics [34], exhaust after-treatment [35], and dilution conditions such as dilution ratio, temperature and relative humidity of the dilution air [36]. However, Rönkkö et al. [9] reported that their formation was insensitive to the fuel sulfur content, dilution air temperature, and relative humidity of ambient air.

Nucleation, condensation and coagulation may change the particle size distribution during the exhaust gas sampling [37]. In this study, the exhaust gas sample was diluted at two stages in order to decrease the particle concentration of the sample for the EEPS. The first dilution was made with heated air (150 °C) in order to prevent the condensation of ambient moisture to sampling lines. However, the first dilution was not sufficiently hot to the prevention of nucleation mode formation. According to Vaaraslahti et al. [38], the nucleation mode evaporates completely when an exhaust sample is heated enough. Thus, the authors of this paper believe the nucleation mode formation could have been avoided if a thermodenuder [39] was adopted during the PN measurement.

Unlike the nucleation mode, the accumulation mode is not sensitive to dilution conditions. [35,40] Accumulation mode particles are formed in the cylinder, when either the fuel or the remnants of lubricating oil do not burn completely during combustion.

Despite the complex nature of nucleation mode, the PN averages calculated from the EEPS scans were found to remain fairly constant, mostly, and be repetitious in this study. The variation of the particle numbers between the three consecutive one-minute EEPS scans can be seen in Fig. 8. The average values were calculated from the recordings of those three EEPS measurement channel, where the PN peaked with different fuels at full load at rated speed.

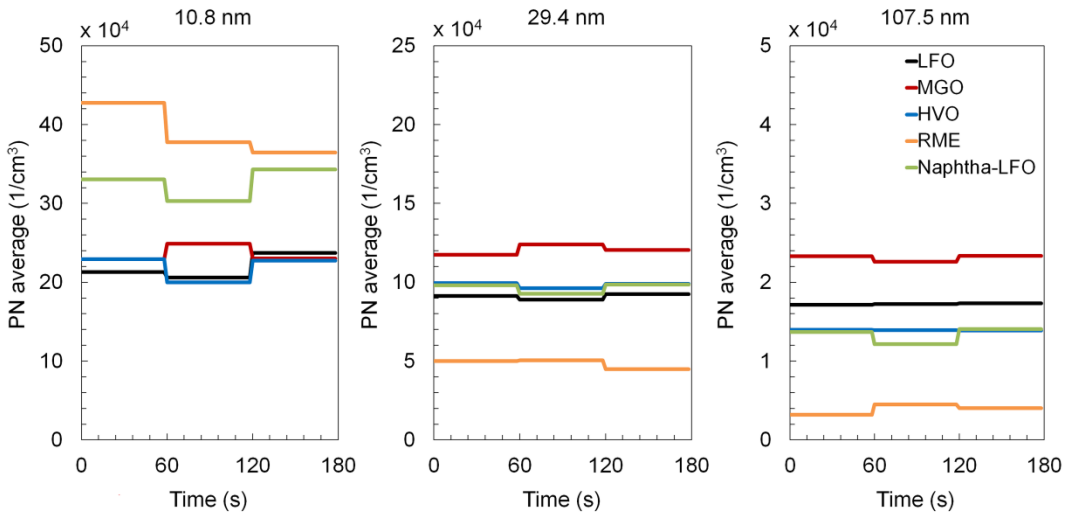

Fig. 8. The variation of the average particle number between the three consecutive one-minute EEPS scans at the three EEPS channels (10.8 nm, 29.4 nm and 107.5 nm).

The physical properties of the liquid fuel tend to control fuel spray characteristics while the fuel composition determines the pathways of chemical reactions during combustion [11]. Besides the fuel sulfur content, particle formation is also influenced by other fuel characteristics such as the fuel density [41,42], viscosity [43,44], and cetane number [45,46]. The start of injection is determined by the fuel density, viscosity, and compressibility. After the injection has started, fuel cetane number determines the moment when combustion starts. Higher fuel density and viscosity lead to an advanced start of injection. A higher cetane number leads to a shortened ignition delay plus advanced combustion. [47]. Too viscous fuel increases pumping losses in the injection system and the injection pressure at the pump end may increase when conventional in-line pumps are adopted. All this may cause disruptions in the combustion process. [48,49]. Higher fuel density and viscosity may lead to incomplete combustion due to poor fuel atomization. Therefore, the soot emission will increase. [50].

In this study, MGO had the second highest density and highest viscosity, which may partly explain why MGO generated the highest TPN at all loads at rated speed even though the cetane number was quite high. At intermediate speed with kerosene, on the other hand, the lowest density and viscosity did not

304 compensate for the effect of the lowest cetane number on clearly the highest TPN. RME had the highest
305 density and second highest viscosity, but the particle numbers within the size range of 37 to 200 nm were
306 still the lowest. However, RME contained approx. 10% oxygen which usually results in lower soot and thus
307 lower accumulation mode particles. Naphtha-LFO blend had a slightly lower cetane number and kinematic
308 viscosity than LFO but a clear difference at density that might explain the reduced particle numbers within
309 the size range of 37 to 200 nm relative to LFO.

310 During the combustion, the aromatic content of fuel has a role as precursors of particulates [51–53]
311 although researchers have received divergent results about the effect of the fuel aromatic content on PM
312 emission [42]. Zetterdahl et al. [53] reported that an increase in the aromatic concentration in low-sulfur
313 diesel fuel led to decreased or unchanged number of particles emitted. However, Talibi et al. [54] concluded
314 that the increasing number of methyl branches on the aromatic ring results in an increased PN, and Peña et
315 al. [55] found that the sizes of primary particles decreased with the addition of methyl group(s) on the
316 aromatic ring. The concentrations of aliphatics and oxygenated groups in soot particles were also decreased.
317 They suggested that the combustion of aromatic fuel, if aliphatic chains are present, tends to produce soot
318 with a compact nanostructure. Due to the same propensity, the content of amorphous, oxygenated, and
319 aliphatic carbonaceous materials in the soot may decrease. Therefore, the reactivity with oxygen decreases
320 too. [55]. Nabi et al. [50] concluded that exhaust particle number and mass emission was higher with MGO
321 compared to diesel fuel due to the higher C/H ratio in MGO. Therefore, they assumed that the aromatic
322 content of MGO would also be higher. This expectation was based on the study of Kalligeros et al. [56],
323 who stated that aromatics increase the fuel C/H ratio.

324 In this study, despite the complex nature of nucleation mode PN formation, the favorable PN results
325 of HVO at the size category of 10 nm are assumed to be caused by the almost zero content of polycyclic
326 aromatic hydrocarbons. On the other hand, the difference in PN at the size 10 nm between MGO and
327 reference fuel LFO cannot be explained by the polyaromatics. The kinematic viscosity of MGO was not
328 much higher than it was for the other fuels, and the content of the polycyclic aromatic compound of MGO
329 was 0.9 wt.-%. This is lower than for LFO for which the maximum allowable content of the polyaromatics

330 is 8 wt.-% [19]. MGO (< 100 mg/kg) and kerosene (1000 mg/kg) contained, however, more sulfur than
331 other fuels, kerosene considerably more. Because a higher content of sulfur was available before
332 combustion, more sulfur oxides, mainly SO_2 and a small fraction of SO_3, were present after fuel burning
333 especially in the case of kerosene. The nucleation mode of particles may be caused by sulfuric acid
334 originating from reaction between SO_3 and water vapor [9,38,57,58]. Therefore, the high PN of MGO and
335 especially of kerosene at the size 10 nm was assumed to be caused by the same reaction and thus due to the
336 higher sulfur contents of these fuels.

337 Unlike HVO, RME produced often the most nucleation mode particles. This result is in line with the
338 several studies of other researchers [44,59–61]. Heikkilä et al. [59] suggested that the relatively high share
339 of nucleation mode particles with RME may be due to its content of viscous, high boiling point molecules,
340 triglycerides and glycerol. Moreover, RME also contains ash forming elements, such as alkali metals and
341 metalloids that may contribute significantly to the formation of the nucleation mode particles.

342 The accumulation mode particles, however, were reduced with RME most likely due to oxygen
343 bounded in mono-alkyl-ester molecules. Thus, the more complete combustion was enabled and the more
344 effective soot oxidation was promoted during RME usage compared the usage of other fuels in this study
345 [62,63]. Nyström et al. [64] detected a lower PN around the peak values of 75–116 nm when a high-speed
346 off-road diesel engine was fueled with RME compared to low-sulfur diesel fuel. Earlier studies have also
347 been reported how RME and other FAMEs, either as neat or the blending component, have the similar
348 decreasing effect on accumulation mode particle numbers [59,65,66].

349 The present study was intended for being able to prepare experiments with a medium-speed engine
350 carefully. In a later study, some of the current fuels were used in a medium-speed engine. Significant
351 combustion differences exist as large marine engines has higher stroke-to-bore ratio compared to smaller
352 high-speed engines. Furthermore, large marine engines are operated with lower engine speeds and higher
353 air-to-fuel ratios than the small engines in land use. High stroke-to-bore ratio, and low engine speed gives
354 more time for fuel to combust which promotes soot oxidation. [31]. As presented by Ntziachristos et al.
355 [31], use of the LFO fuel in a marine engine may result to much lower specific mass emissions of particles

compared to the emission limitation intended for road vehicles at some loads. Therefore, the presented PN reductions may be presupposed when the fuels of this study are later intended for marine applications. No parameter optimization was applied with the studied fuels at this first stage to be able to compare the fuels first without any modifications. At the next stages, parameters have to be optimized.

5. Conclusions

This study concentrated on working out how different alternative off-road engine fuels affect the exhaust particle size distributions of a high-speed diesel engine. The examined fuels were a blend of renewable wood-based naphtha and marine low-sulfur LFO, circulation-origin MGO, RME, HVO, and kerosene. LFO worked as baseline fuel. The measurements were performed according to the NRSC test cycle. Based on the obtained results, the following conclusions could be drawn:

- A bimodal shape was detected in all particle size distributions.
- Considering the complex nature of nucleation mode PN formation, no consistent conclusions could be drawn concerning the particle numbers under the size category of 50 nm.
- Except at idle, the particle numbers above 50 nm were the lowest with RME most likely due to oxygen bounded in mono-alkyl-ester molecules.
- Relative to LFO, both naphtha-LFO blend and RME reduced particle numbers above 50 nm-at rated and intermediate speeds.
- Circulation economy based MGO generated the highest total particle number (TPN) at all loads at rated speed, most likely due to the higher fuel sulfur content. At intermediate speed, still higher TPN values were recorded for kerosene, the sulfur content of which was higher by one order of magnitude relative to MGO.
- In terms of TPN at intermediate speed, renewable HVO was more beneficial than LFO. At rated speed, the HVO results were quite similar to those of LFO.

- Concerning the TPN as a whole, the blend of renewable naphtha and LFO was competitive with LFO. At some loads, the blend emitted more particles, at other loads less than LFO.
- MGO and RME were favorable in terms of CO and HC emissions while the lowest NOx emissions were recorded with HVO.
- Smoke emission was negligible for all fuels.

Declarations of interest

None.

Acknowledgements

This study was funded from the European Union's Horizon 2020 research and innovation programme under the grant agreement No 634135 (Hercules-2). The Novia University of Applied Sciences allowed us to use the engine laboratory for this study. The authors wish to thank Dr. Tony Pellfolk and Mr. Holger Sved for this possibility. In addition, the authors wish to thank Mrs. Michaela Hissa, Mrs. Sonja Heikkilä and Ms. Nelli Vanhala for their assistance during the measurement campaigns.

References

[1] Reducing Sulphur Emissions from Ships - The Impact of International Regulation. OECD International Transport Forum; 2016 [accessed 21 Aug 2018]. Available from: https://www.itf-oecd.org/sites/default/files/docs/sulphur-emissions-shipping.pdf

[2] Internal Maritime Organization. Prevention of Air Pollution from Ships, http://www.imo.org/en/OurWork/Environment/PollutionPrevention/AirPollution/Pages/Air-Pollution.aspx; 2018 [cited 17 August 2018].

[3] Sarvi A, Lyyränen J, Jokiniemi J, Zevenhoven R. Particulate emissions from large-scale medium-speed diesel engines: 1. Particle size distribution. Fuel Process Technol 2011;92(10):1855–61. https://dx.doi.org/10.1016/j.fuproc.2011.04.031.

[4] Zetterdahl M, Moldanová J, Pei X, Pathak RK, Demirdjian B. Impact of the 0.1% fuel sulfur content limit in SECA on particle and gaseous emissions from marine vessels. Atmos Environ 2016;145:338–45. https://dx.doi.org/10.1016/j.atmosenv.2016.09.022.

[5] Kittelson DB. Engines and nanoparticles: a review. J Aerosol Sci 1998;(5–6);575–88. https://dx.doi.org/10.1016/S0021-8502(97)10037-4.

[6] Rönkkö T, Virtanen A, Vaaraslahti K, Keskinen J, Pirjola L, Lappi M. Effect of dilution conditions and driving parameters on nucleation mode particles in diesel exhaust: Laboratory and on-road study. Atmos. Environ. 2006;40(16):2893–901. https://doi.org/10.1016/j.atmosenv.2006.01.002.

[7] Filippo AD, Maricq MM. Diesel nucleation mode particles: Semivolatile or solid?. Environ Sci Technol 2008;42(21):7957–62. https://dx.doi.org/10.1021/es8010332.

[8] Lähde T, Rönkkö T, Virtanen A, Solla A, Kytö M, Söderström C., et al. Dependence between nonvolatile nucleation mode particle and soot number concentrations in an EGR equipped heavy-duty diesel engine exhaust. Environ Sci Technol 2010;44(8):3175–80.

[9] Rönkkö T, Virtanen A, Kannosto J, Keskinen J, Lappi M, Pirjola L. Nucleation mode particles with a nonvolatile core in the exhaust of a heavy duty diesel vehicle. Environ Sci Technol 2007;41(18):6384–9. https://dx.doi.org/10.1021/es0705339.

[10] Zhang Y, Ghandhi J, Rothamer D. Comparisons of particle size distribution from conventional and advanced compression ignition combustion strategies. Int J Engine Res 2018;19(7):699–717. https://doi.org/10.1177/1468087417721089.

[11] Eastwood P. Particulate Emissions from Vehicles. Chichester: John Wiley & Sons Ltd; 2008.

[12] Millo F, Rafigh M, Andreata M, Vlachos T, Arya P, Miceli P. Impact of high sulfur fuel and de-sulfation process on a close-coupled diesel oxidation catalyst and diesel particulate filter. Fuel 2017;198:58–67. https://dx.doi.org/10.1016/j.fuel.2017.01.006.

[13] EU Regulation 2016/1628. Regulation of the European Parliament and of the Council on requirements relating to gaseous and particulate pollutant emission limits and type-approval for internal combustion engines for non-road mobile machinery; 2016 [accessed 17 Aug 2018].

433 Available from: https://eur-lex.europa.eu/legal-content/EN/TXT/PDF/?uri=CELEX:32016R1628&
434 from=EN
435 [14] Kalli J, Karvonen T, Makkonen T. Sulphur Content in Ships Bunker Fuel in 2015 - A study on the
436 impacts of the new IMO regulations and transportation costs. Helsinki: Publications of the Ministry
437 of Transport and Communications; 2009 [accessed 17 Aug 2018]. Available from:
438 https://www.lvm.fi/documents/20181/817543/Julkaisuja+31-2009/cfb920d0-d1c5-4c4f-94e2-
439 7a92e58adc9d?version=1.0
440 [15] Jääskeläinen S. Alternative transport fuels infrastructure - Finland´s national plan. Helsinki, Finland:
441 Publications of the Ministry of Transport and Communications; 2017 [accessed 17 Aug 2018].
442 Available from: https://julkaisut.valtioneuvosto.fi/bitstream/handle/10024/80230/Report%205-
443 2017.pdf?sequence=1
444 [16] Florentinus A, Hamelinck C, van den Bos A, Winkel R, Cuijpers M. Potential of biofuels for
445 shipping - Final Report. Prepared by Ecofys for European Maritime Safety Agency (EMSA); 2012
446 [accessed 17 Aug 2018]. Available from:
447 https://www.ecofys.com/files/files/ecofys_2012_potential_of_biofuels_in_shipping_02.pdf
448 [17] Niemi S, Vauhkonen V, Mannonen S, Ovaska T, Nilsson O, Sirviö K, et al. Effects of wood-based
449 renewable diesel fuel blends on the performance and emissions of a non-road diesel engine. Fuel
450 2016;186:1–10. https://dx.doi.org/10.1016/j.fuel.2016.08.048.
451 [18] Fernandes G, Fuschetto J, Filipi Z, Assanis D, McKee H. Impact of military JP-8 fuel on heavy-duty
452 diesel engine performance and emissions. Proc Inst Mech Eng Part D: J Automobile Eng
453 2007;221(8):957–70. http://dx.doi.org/10.1243/09544070JAUTO211.
454 [19] SFS-EN 590:2013. Automotive fuels. Diesel. Requirements and test methods. Finnish Petroleum
455 Federation; 2013.
456 [20] Aatola H, Larmi M, Sarjovaara T, Mikkonen S. Hydrotreated Vegetable Oil (HVO) as a Renewable
457 Diesel Fuel: Trade-off between NO_x, Particulate Emission, and Fuel Consumption of a Heavy Duty
458 Engine. SAE Int J Engines 2009;1(1):1251–62. https://dx.doi.org/10.4271/2008-01-2500.

[21] Product data sheet. Aviation Jet Fuel Jet A-1. Espoo: Neste Oyj; 2015.

[22] Wang X, Grose MA, Caldow R, Osmondson BL, Swanson JJ, Chow JC, et al. Improvement of Engine Exhaust Particle Sizer (EEPS) Size Distribution Measurement – II. Engine Exhaust Aerosols. J Aerosol Sci 2016;92:83–94. https://doi.org/10.1016/j.jaerosci.2015.11.003.

[23] Dieselnet, http://www.dieselnet.com; 2018 [accessed 17 August 2018].

[24] Kittelson DB, Watts WF, Johnson JP. On-road and laboratory evaluation of combustion aerosols, Part1: Summary of diesel engine results. J Aerosol Sci 2006;37(8):913–30. https://dx.doi.org/10.1016/j.jaerosci.2005.08.005.

[25] Thiruvengadam A, Besch MC, Yoon S, Collins J, Kappanna H, Carder DK, et al. Characterization of particulate matter emissions from a current technology natural gas engine. Environ Sci Technol 2014;48(14):8235–42. https://dx.doi.org/10.1021/es5005973.

[26] Pirjola L, Karjalainen P, Heikkilä J, Saari S, Tzamkiozis T, Ntziachristos L, et al. Effects of fresh lubricant oils on particle emissions emitted by a modern gasoline direct injection passenger car. Environ Sci Technol 2015;49(6):3644–52. https://dx.doi.org/10.1021/es505109u.

[27] Karjalainen P, Pirjola L, Heikkilä J, Lähde T, Tzamkiozis T, Ntziachristos L, et al. Exhaust particles of modern gasoline vehicles: A laboratory and an on-road study. Atmos Environ 2014;97:262–70. http://dx.doi.org/10.1016/j.atmosenv.2014.08.025.

[28] Anderson M, Salo K, Hallquist ÅM, Fridell E. Characterization of particles from a marine engine operating at low loads. Atmos Environ 2015;101:65–71. http://dx.doi.org/10.1016/j.atmosenv.2014.11.009.

[29] Pirjola L, Rönkkö T, Saukko E, Parviainen H, Malinen A, Alanen J, et al. Exhaust emissions of non-road mobile machine: Real-world and laboratory studies with diesel and HVO fuels. Fuel 2017;202:154–64. https://dx.doi.org/10.1016/j.fuel.2017.04.029.

[30] Ovaska T, Niemi S, Katila T, Nilsson O. Exhaust particle size distributions of a non-road diesel engine in an endurance test. Agronomy Research 2018;16(S1):1159–68. https://dx.doi.org/10.15159/AR.18.087.

485 [31] Ntziachristos L, Saukko E, Lehtoranta K, Rönkkö T, Timonen H, Simonen P, et al. Particle
486 emissions characterization from a medium-speed marine diesel engine with two fuels at different
487 sampling conditions. Fuel 2016;186:456–65. https://dx.doi.org/10.1016/j.fuel.2016.08.091.
488 [32] Nousiainen P, Niemi S, Rönkkö T, Karjalainen P, Keskinen J, Kuuluvainen H, et al. Effect of
489 injection parameters on exhaust gaseous and nucleation mode particle emissions of a Tier 4i nonroad
490 diesel engine. SAE Technical Paper 2013; 2013-01-2575. https://doi.org/10.4271/2013-01-2575.
491 [33] Lähde T, Rönkkö T, Happonen M, Söderström C, Virtanen A, Solla A, et al. Effect of fuel injection
492 pressure on a heavy-duty diesel engine nonvolatile particle emission. Environ Sci Technol
493 2011;45(6):2504–9. https://doi.org/10.1021/es103431p.
494 [34] Vaaraslahti K, Keskinen J, Giechaskiel B, Solla A, Murtonen T, Vesala H. Effect of lubricant on the
495 formation of heavy-duty diesel exhaust nanoparticles. Environ Sci Technol 2005;39(21):8497–504.
496 [35] Maricq MM, Chase RE, Xu N, Laing PM. The effects of the catalytic converter and fuel sulfur level
497 on motor vehicle particulate matter emissions: light duty diesel vehicles. Environ Sci Technol
498 2002;36(2):283–89.
499 [36] Mathis U, Ristimaki J, Mohr M, Keskinen J, Ntziachristos L, Samaras Z, Mikkanen P. Sampling
500 conditions for the measurement of nucleation mode particles in the exhaust of a diesel vehicle.
501 Aerosol Sci Technol 2004;38(12):1149–60.
502 [37] Barrios CC, Domínguez-Sáez A, Rubio JR, Pujadas M. Development and evaluation of on-board
503 measurement system for nanoparticle emissions from diesel engine. Aerosol Sci Technol
504 2011;45(5):570–80. https://doi.org/10.1080/02786826.2010.550963.
505 [38] Vaaraslahti K, Virtanen A, Ristimäki J, Keskinen J. Nucleation mode formation in heavy-duty diesel
506 exhaust with and without a particulate filter. Environ Sci Technol 2004;38(18):4884–90.
507 https://dx.doi.org/10.1021/es0353255.
508 [39] An WJ, Pathak RK, Lee BH, Pandis SN. Aerosol volatility measurement using an improved
509 thermodenuder: Application to secondary organic aerosol. J Aerosol Sci 2007;38(3):305–14.
510 https://doi.org/10.1016/j.jaerosci.2006.12.002.

[40] Kittelson DB, Watts W, Johnson J. Diesel aerosol sampling methodology; CRC E-43 Final Report; University of Minnesota: Minneapolis, 2002.

[41] Szybist JP, Song J, Alam M, Boehman AL. Biodiesel combustion, emissions and emission control. Fuel Process Technol 2007;88(7):679–91. https://dx.doi.org/10.1016/j.fuproc.2006.12.008.

[42] Bach F, Tschöke H, Simon H. Influence of Alternative Fuels on Diesel Engine Aftertreatment. In: 7th International Colloquium Fuels - mineral oil based and alternative fuels 14–15th January, Ostfildern, Germany; 2009.

[43] Mathis U, Mohr M, Kaegi R, Bertola A, Boulouchos K. Influence of diesel engine combustion parameters on primary soot particle diameter. Environ Sci Technol 2005;39(6):1887–92. https://dx.doi.org/10.1021/es049578p.

[44] Tsolakis A. Effects on particle size distribution from the diesel engine operating on RME-biodiesel with EGR. Energy & Fuels 2006;20(4):1418–24. https://dx.doi.org/10.1021/ef050385c.

[45] Li R, Wang Z, Ni P, Zhao Y, Li M, Li L. Effects of cetane number improvers on the performance of diesel engine fuelled with methanol/biodiesel blend. Fuel 2014;128:180–7. https://dx.doi.org/10.1016/j.fuel.2014.03.011.

[46] Alrefaai MM, Peña GDG, Raj A, Stephen S, Anjana T, Dindi A. Impact of dicyclopentadiene addition to diesel on cetane number, sooting propensity, and soot characteristics. Fuel 2018;216:110–20. http://dx.doi.org/10.1016/j.fuel.2017.11.145.

[47] Kegl B, Kegl M, Pehan S. Green diesel engine. Biodiesel usage in diesel engines. London: Springer-Verlag; 2013.

[48] Guibet JC. Fuels and Engines: Technology, Energy, Environment. Vol 1. Paris: Éditions Technip; 1999.

[49] Kalghatgi G. Fuel/Engine Interactions. Warrendale, PA: SAE International; 2014.

[50] Nabi MdN, Brown R, Ristovski Z, Hustad J. A comparative study of the number and mass of fine particles emitted with diesel fuel and marine gas oil (MGO). Atmos Environ 2012;57:22–8. https://dx.doi.org/10.1016/j.atmosenv.2012.04.039.

[51] Ntziachristos L, Samaras Z, Pistikopoulos P, Kyriakis N. Statistical analysis of diesel fuel effects on particle number and mass emissions. Environ Sci Technol 2000;34(24):5106–14. https://dx.doi.org/10.1021/es000074a.

[52] Tree DR, Svensson KI. Soot processes in compression ignition engines. Prog Energ Combust 2007;33(3):272–309. https://dx.doi.org/10.1016/j.pecs.2006.03.002.

[53] Zetterdahl M, Salo K, Fridell E, Sjöblom J. Impact of Aromatic Concentration in Marine Fuels on Particle Emissions. J Marine Sci Appl 2017;16(3):352–61. https://dx.doi.org/10.1007/s11804-017-1417-7.

[54] Talibi M, Hellier P, Ladommatos N. Impact of increasing methyl branches in aromatic hydrocarbons on diesel engine combustion and emissions. Fuel 2018;216:579–88. https://dx.doi.org/10.1016/j.fuel.2017.12.045.

[55] Peña GDG, Alrefaai MM, Yang SY, Raj A, Brito JL, Stephen S, et al. Effects of methyl group on aromatic hydrocarbons on the nanostructures and oxidative reactivity of combustion-generated soot. Combust Flame 2016;172:1–12. https://dx.doi.org/10.1016/j.combustflame.2016.06.026.

[56] Kalligeros S, Zannikos F, Stournas S, Lois E, Anastopoulos G, Teas C, et al. An investigation of using biodiesel/marine diesel blends on the performance of a stationary diesel engine. Biomass and Bioenergy 2003;24(2):141–9. http://dx.doi.org/10.1021/es0515452.

[57] Arnold F, Pirjola L, Aufmhoff H, Schuck T, Lähde T, Hämeri K. First gaseous sulphuric acid measurements in automobile exhaust: Implications for volatile nanoparticle formation. Atmos Environ 2006;40(37):7079–105. http://dx.doi.org/10.1016/j.atmosenv.2006.06.038.

[58] Biswas S, Hu S, Verma V, Herner JD, Robertson WH, Ayala A, et al. Physical properties of particulate matter (PM) from late model heavy-duty diesel vehicles operating with advanced PM and NO_x emission control technologies. Atmos Environ 2008;42(22):5622–34. http://dx.doi.org/10.1016/j.atmosenv.2008.03.007.

561 [59] Heikkilä J, Virtanen A, Rönkkö T, Keskinen J, Aakko-Saksa P, Murtonen T. Nanoparticle emissions
562 from a heavy-duty engine running on alternative diesel fuels. Environ Sci Technol
563 2009;43(24):9501–6. http://dx.doi.org/10.1021/es9013807.
564 [60] Jayaram V, Agrawal H, Welch WA, Miller JW, Cocker III DR. Real-time gaseous, PM and ultrafine
565 particle emissions from a modern marine engine operating on biodiesel. Environ Sci Technol
566 2011;45(6):2286–92. http://dx.doi.org/10.1021/es1026954.
567 [61] Lackey LG, Paulson SE. Influence of feedstock: Air pollution and climate-related emissions from a
568 diesel generator operating on soybean, canola, and yellow grease biodiesel. Energy & Fuels
569 2011;26(1): 686–700. https://dx.doi.org/10.1021/ef2011904.
570 [62] Yang HH, Chien SM, Lo MY, Lan JCW, Lu WC, Ku YY. Effects of biodiesel on emissions of
571 regulated air pollutants and polycyclic aromatic hydrocarbons under engine durability testing. Atmos
572 Environ 2007;41(34):7232–40. https://dx.doi.org/10.1016/j.atmosenv.2007.05.019.
573 [63] Lapuerta M, Armas O, Rodriguez-Fernandez J. Effect of biodiesel fuels on diesel engine emissions.
574 Progr Energy Combust Sci 2008;34(2):198–223. https://dx.doi.org/10.1016/j.pecs.2007.07.001.
575 [64] Nyström R, Sadiktsis I, Ahmed TM, Westerholm R, Koegler JH, Blomberg A, et al. Physical and
576 chemical properties of RME biodiesel exhaust particles without engine modifications. Fuel
577 2016;186:261–9. https://dx.doi.org/10.1016/j.fuel.2016.08.062.
578 [65] Jung H, Kittelson DB, Zachariah MR. Characteristics of SME biodiesel-fueled diesel particle
579 emissions and the kinetics of oxidation. Environ Sci Technol 2006;40(16):4949–55.
580 http://dx.doi.org/10.1021/es0515452.
581 [66] Rounce P, Tsolakis A, York APE. Speciation of particulate matter and hydrocarbon emissions from
582 biodiesel combustion and its reduction by aftertreatment. Fuel 2012;96:90–9.
583 https://dx.doi.org/10.1016/j.fuel.2011.12.071.